Dissociation Cross Sections and Rates for Nitrogen

David W. Schwenke
NASA Ames Research Center
MS T27B
Moffett Field, CA 94035-1000 U.S.A.

david.w.schwenke@nasa.gov

ABSTRACT

The N, N_2 system is studied to yield rate coefficients and cross sections for molecular dissociation under conditions important for assessing nonequilibrium heating of hypersonic vehicles. First principle calculations are used to generate realistic nuclear interaction potentials, and these are used with accurate molecular dynamics to yield the fundamental data required for a rigorous treatment of nonequilibrium chemistry.

1.0   INTRODUCTION

Space-craft entering planetary atmospheres must withstand significant heating as the aero braking arising from the interaction with the atmosphere converts kinetic energy of the craft into chemical energy. If the entry speed is low enough, *e.g.* less than about 11 Km/s, which is the entry speed for the space shuttle, the rates of the chemical processes are sufficiently fast that chemical equilibrium is an adequate model to describe the role of chemistry in the flow equations and to model the heating. When chemistry is in equilibrium, the chemical composition and chemical energy is determined by a single parameter, the local temperature.

When entry speeds increase, the chemical time scales and flow time scales become more similar, and reliable predictions of heating are no longer possible without explicitly dealing with nonequilibrium chemistry. For example, the Stardust return capsule entered the earth's atmosphere at about 12.6 Km/s, and

Figure 1 Stardust entering Earth's atmosphere

nonequilibrium N_2 dissociation played a significant role in predicting the shock heating. At even higher entry speeds, such as lunar return, nonequilibrium ionization is expected to play an important role. However, in contrast to the equilibrium situation where the local temperature controls everything, a reliable description of nonequilibrium chemistry is much, much more complicated. In the past,[1] the solution to the nonequilibrium chemistry problem has been to build models with additional variables, such specific species concentrations and internal state distribution function

		Form Approved	

Report Documentation Page

Form Approved
OMB No. 0704-0188

Public reporting burden for the collection of information is estimated to average 1 hour per response, including the time for reviewing instructions, searching existing data sources, gathering and maintaining the data needed, and completing and reviewing the collection of information. Send comments regarding this burden estimate or any other aspect of this collection of information, including suggestions for reducing this burden, to Washington Headquarters Services, Directorate for Information Operations and Reports, 1215 Jefferson Davis Highway, Suite 1204, Arlington VA 22202-4302. Respondents should be aware that notwithstanding any other provision of law, no person shall be subject to a penalty for failing to comply with a collection of information if it does not display a currently valid OMB control number.

1. REPORT DATE **SEP 2009**	2. REPORT TYPE **N/A**	3. DATES COVERED **-**	
4. TITLE AND SUBTITLE **Dissociation Cross Sections and Rates for Nitrogen**		5a. CONTRACT NUMBER	
		5b. GRANT NUMBER	
		5c. PROGRAM ELEMENT NUMBER	
6. AUTHOR(S)		5d. PROJECT NUMBER	
		5e. TASK NUMBER	
		5f. WORK UNIT NUMBER	
7. PERFORMING ORGANIZATION NAME(S) AND ADDRESS(ES) **NASA Ames Research Center MS T27B Moffett Field, CA 94035-1000 U.S.A.**		8. PERFORMING ORGANIZATION REPORT NUMBER	
9. SPONSORING/MONITORING AGENCY NAME(S) AND ADDRESS(ES)		10. SPONSOR/MONITOR'S ACRONYM(S)	
		11. SPONSOR/MONITOR'S REPORT NUMBER(S)	

12. DISTRIBUTION/AVAILABILITY STATEMENT
Approved for public release, distribution unlimited

13. SUPPLEMENTARY NOTES
See also ADA562449. RTO-EN-AVT-162, Non-Equilibrium Gas Dynamics - From Physical Models to Hypersonic Flights (Dynamique des gaz non- equilibres - Des modeles physiques jusqu'au vol hypersonique)., The original document contains color images.

14. ABSTRACT
The N, N2 system is studied to yield rate coefficients and cross sections for molecular dissociation under conditions important for assessing nonequilibrium heating of hypersonic vehicles. First principle calculations are used to generate realistic nuclear interaction potentials, and these are used with accurate molecular dynamics to yield the fundamental data required for a rigorous treatment of nonequilibrium chemistry.

15. SUBJECT TERMS

16. SECURITY CLASSIFICATION OF:			17. LIMITATION OF ABSTRACT	18. NUMBER OF PAGES	19a. NAME OF RESPONSIBLE PERSON
a. REPORT **unclassified**	b. ABSTRACT **unclassified**	c. THIS PAGE **unclassified**	**SAR**	**18**	

Standard Form 298 (Rev. 8-98)
Prescribed by ANSI Std Z39-18

parameters. The problem with this solution is that the model can contain many uncertainties that can be extremely difficult to quantify. One often ignored problem is that the phenomenological nature of the model causes the input rate coefficients to lose their physical meaning, thus it is difficult to judge how one relates data obtained from experiments designed to measure rate data to the quantities required for the model. One is then left with validation of the models by comparing to experimental data from laboratory experiments that only approximately mimic flight conditions, or by comparing to the very sparse flight data. In either case, the harsh conditions involved make the interpretation and exact characterization of the data fiendishly difficult and unambiguous model improvement is impossible.

Under the support of the NASA Fundamental Aeronautics Hypersonic research program, the computational chemists at NASA Ames have embarked on an alternate solution, namely the characterization of nonequilibrium chemistry from first principles. In this work we will focus our attention on the dissociation of N_2 by means of collisions with N atoms and N_2 molecules.

2.0   CHEMISTRY BASED FORMALISM

The theoretical formulation encompasses vast length scales, from macroscopic vehicle dimensions to atomistic dimensions. The makes a rigorous complete formulation impossible. Fortunately there are numerous physical approximations which are quite reliable that allow us to decouple various length scales. Thus we will take a divide and conquer approach.

We start at the atomistic level. Molecules and atoms move very fast and the range of inter-molecular interactions is fairly short range, thus the time between collisions is much greater than the duration of a typical collision. Thus, to a very good approximation, we can start by considering our universe to consist of two particles that undergo a collision in isolation from all other particles.

2.1   N+N

We consider initially two nitrogen atoms. How do we describe their motion? This by itself is a difficult task, principally because the forces between particles is due not only to the nuclei, but also to the electrons. Thus we must explicitly treat the electrons and nuclei of the colliding particles. This leads to high dimensionality problems: for example, a nitrogen atom has seven electrons, so the treatment of two N atoms is a problem in $3\times2\times(1+7)=48$ dimensions.

Before we go on and describe how we proceed, it should be noted that nuclear spin plays a non-trivial role.[2] The nuclear spin leads to very small corrections to the forces between the particles, thus can be ignored when determining the interactions. However, since a N nucleus has a nuclear spin 1, it is a boson, and thus only spin-electronic-ro-vibrational wavefunctions that are totally symmetric are present in nature. Thus for the ground electronic state of N_2, out of the 9 possible nuclear spin couplings, only 3 appear with odd rotational quantum numbers, and only 6 appear with even quantum numbers. In spectra, this is manifested by a 2:1 alternation in the intensities of the different rotational levels. This complication on the kinetics can be included in a straightforward, rigorous manner, but introduces additional complications into the formalism[3] which will be neglected in the present work to make the presentation more transparent.

We will now speak of nuclear spin no more and go on to the treatment of the nuclei and electrons. A problem of this sort is not feasible to solve exactly, thus we must resort to further approximations. Fortunately nature is kind, and the ratio of N nuclear mass to an electron mass is about 2.6×10^4, which enables us to obtain excellent results if we consider the nuclei to be stationary when we treat the electrons. [2] For N_2, this enables us to reduce the problem to one in $3\times2=6$ dimensions (the nuclear problem), and many in $3\times2\times7=42$ dimensions (the electron problem).

The electron problem remains a very formidable problem, but we again have several mitigating factors. The electron motion is governed by the laws of quantum mechanics, which simply put leads to probability distribution functions for particles, and the probability distribution goes hand in hand with an average energy, with the energy levels fixed by boundary conditions and Planck's constant. The first mitigating factor is that all electrons are indistinguishable, which means that a mean field approximation can provide a reasonable starting point for obtaining a solution. In the mean field approximation, the motion of one electron, a 3 dimensional problem, is found from using the average position of all the remaining electrons. This leads to an iterative refinement of the orbitals describing the probability distribution of an electron's position. This level of calculation is quite feasible for very large systems (hundreds of atoms). To go beyond this level of approximation, which is required for the accuracy we need, we can consider two electrons at a time, with the motion of the remaining electrons being averaged over. This is more expensive, and is still not accurate enough. The most reliable method used today is to treat the motion of two electrons explicitly, but allow the other electrons to interact via functional restrictions. Very efficient computer codes have been written to solve for this problem, but still solutions are practical only up to half a dozen or so atoms in the system.

The second mitigating factor is that the light mass of the electrons means that the spacing of energy levels is very great. Thus, to a very good degree of approximation, we need to consider only the lowest possible energy level of the electrons. Nonetheless, a calculation of the electron energy level for a single nuclear geometry requires the solution of a non-linear problem with millions of unknowns.

By splitting the nuclear and electron problems, we have enabled the solution of the electron problem without consideration of the nuclear motion, but at the expense of having to solve repeatedly the electron problem for each position the nuclei take during the collision. This is, of course, another formidable problem, because the nuclei sample an infinite number of positions during a collision. To circumvent this
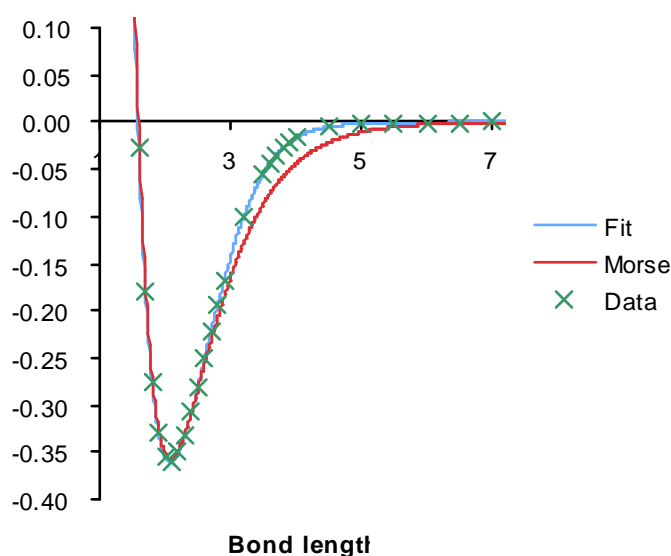
Figure 2: Calculated and fitted potential energy curve of N_2 and simple Morse model.

problem, we carefully select a set of nuclear geometries which we think well characterize the set of geometries encountered, and solve for the electronic energy at these points. These points are then fit to some analytic function in order to interpolate/extrapolate the energies. In Figure 2 we show such a result for N_2. We show the data, the fitting function, and finally a Morse potential. The Morse potential is a simple three parameter function which has simple vibrational energy levels, while the fit is a 14 parameter

analytic function. The fit reproduces the data very well, and the Morse function does a good job of representing the data until about half way up to dissociation limit, but then starts to give rise to large deviations. Since in the present work, N_2 dissociation is of interest, it is likely that the Morse potential would not provide a good basis for further work. It is interesting to note that while the Morse potential appears to have longer range, *i.e.* it seems to decay more slowly than the fit, the fit is actually of longer range, for it approaches the asymptotic limit as r^{-6}, where r is the N_2 bond length, while the Morse potential approaches the asymptotic limit exponentially.[2] This has profound implications for the number of bound ro-vibrational levels of N_2. Also note the higher density of data points in the vicinity of a bound length of 4. This was required to ensure the analytic representation behaved properly as the potential evolved from its asymptotic long range behaviour to the short range bonding interaction. This effected the number of bound ro-vibrational levels, and will be discussed further below.

Let us now move on to the treatment of nuclear motion. After the electrons have been taken care of, we have 6 degrees of freedom remaining. By transforming to a new set of cartesian position vectors, one that specifies the center of mass of the N_2 molecule, and the other which specifies the length and direction of the bond, we can simplify the problem, since the potential energy curve does not depend on the center of mass cartesians. This reduces the problem to one in three dimensions, since the center of mass motion is easily solved for and furthermore plays no role in this study. By transforming the cartesians specifying the length and direction of the bond into spherical polar coordinates, we can further simplify the problem, since the potential energy curve only depends on r, the length of this vector, and partially separate vibration and rotational motion.

Thus we now have a rotational and vibrational problem to solve. How do we do this? By virtue of their small mass, electrons must be treated by quantum mechanics. As particles get heavier, gradually classical mechanics becomes more valid. Now since the mass of an N atom is about 2.6×10^4 times greater than an electron's mass, it is tempting to consider using classical mechanics. This is because classical mechanics is local while quantum mechanics is non-local and hence much more expensive. Thus let us consider three ways for treating nuclear dynamics: classical mechanics, old quantum mechanics, and quantum mechanics.

In a classical mechanical calculation, one determines the time evolution of a set of coordinates q_i, and conjugate momentum p_i. The time evolution is governed by Hamilton's equations[4]

$$\dot{q}_i = \frac{\partial H}{\partial p_i}, \ \dot{p}_i = -\frac{\partial H}{\partial q_i}$$

where the Hamiltonian for a 1-d vibrator, for example, is

$$H = \frac{p^2}{2m} + V(q)$$

where m is the reduced mass for the vibrator, $m_N/2$ for N_2. The solution of these equations, while interesting by themselves, do not appear helpful in the situation of approximating quantum mechanics, for nothing about quantization of energy appears. To proceed, we must invoke the premises of so-called "old" quantum mechanics. [5] In this procedure, we take the above equations and transform to a new set of variables, called action-angle variables. These variables are special in that the new momenta, the actions, are constant in time, *i.e.* the new Hamiltonian has no dependence on the variables conjugate to the actions, the angle variables. Then the quantization rule is that the only allowed values of the actions are half integral multiples of $\hbar$, but the particles still follow regular trajectories: the angle variables progress in straight lines. The action-angle variables can be determined analytically for a few 1-d problems, but must be determined numerically for most systems of interest.

We now compare this to quantum mechanics. Now we must solve a eigenvalue eigenvector problem:

$$\hat{H}\Psi_n = E_n \Psi_n$$

where the quantum mechanical Hamiltonian operator is built from simple rules from the classical Hamiltonian, $|\Psi_n|^2$ gives the probability density, and E_n is the energy. For the 1-d vibrator, the Hamiltonian operator is

$$-\frac{\hbar^2}{2m}\frac{\partial^2}{\partial q^2} + V(q).$$

How do the predicted energies between the old and new quantum mechanics compare? For a diatomic molecule, like N_2, the agreement is quite good. For example, the rotational energy levels from quantum mechanics are $\dfrac{j(j+1)\hbar^2}{2mr^2}$, where j is the integral rotational quantum number and r is the bond length, while the rotational energy levels from old quantum mechanics are $\dfrac{\left(j+\frac{1}{2}\right)^2\hbar^2}{2mr^2}$. The difference between these two results is only $\dfrac{\hbar^2}{8mr^2}$ which is pretty small considering how large m is. For vibration, the situation is similar: for a Morse oscillator and Harmonic oscillator, the old quantum mechanics gives the same answer as does quantum mechanics, provided the domain of the bond length is $-\infty$ to $+\infty$, a not to restrictive assumption for the current value of m. Thus we see that the old quantum mechanics works quite well for N_2.

Now consider what happens when one couples vibration and rotation. One finds that the net effect is to add the term $\dfrac{\left(j+\frac{1}{2}\right)^2\hbar^2}{2mr^2}$ to the vibrational potential. It should be noted that the attraction of a Morse potential, namely that action-angle variables can be determined analytically, does not hold when the molecule rotates. The term $\dfrac{\left(j+\frac{1}{2}\right)^2\hbar^2}{2mr^2}$ that is added to the potential precludes analytic action-angle variables.
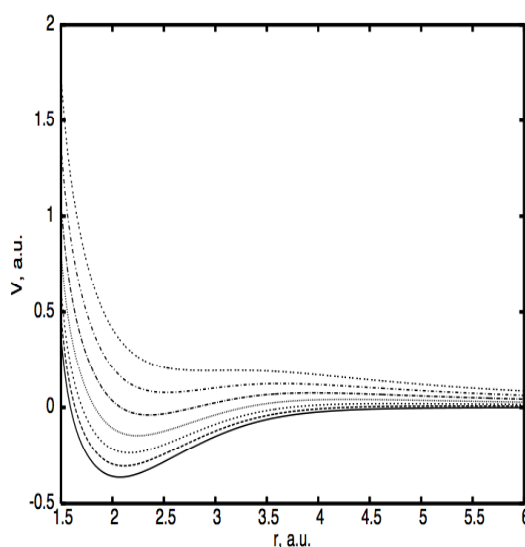

Figure 3: Potential curve of N_2 for j=0,20,40,..

The effect of rotation on the potential of N_2 is shown in Figure 3. In general, as j increases, the potential minimum decreases in depth and gets pushed to larger r. An interesting situation occurs when the potential minimum rises to the point it is no longer the global minimum, but simply a local minimum. In this case, quantum mechanically, there is probability of finding the particle inside of the centrifugal barrier as well as outside the barrier. Physically, if the particle started inside the centrifugal barrier, the probability of finding it there will decay exponentially with time. These levels are called quasi-bound levels, predissociated levels, or resonant levels, depending on the scientific field in which they are discussed. Finally, eventually as j becomes larger, the potential will become purely repulsive, and no more bound or quasi-bound levels will exist.

In Figure 4, we show the range of v and j for which there are bound or quasibound levels. For $j=0$, there are bound vibrational levels up to 60, whereas for $v=0$, there are bound rotational levels up to j about 210, and quasibound levels continuing up to $j=279$. In our initial calculations on N_2, we noticed a rather odd bulge on a plot of this type in the vicinity of $v=50$. This turned out to be due to additional bound states coming from incorrect behaviour of the potential of Figure 2 in the region around 4 bohr. When we added the additional points around 4 bohr and improved the analytic representation in this region, the bulge went away, and we were left with a plot very like Figure 4. The potential used to generate the data shown in this figure is obtained not from the potential of Figure 2, but rather an accurate potential determined from fitting spectroscopic data for N_2.[6] The differences between these potentials is not that great, but certainly the one based on experiment is more accurate, so we will use it. The number of bound and quasibound levels for N_2 is 9390 from old quantum mechanics.
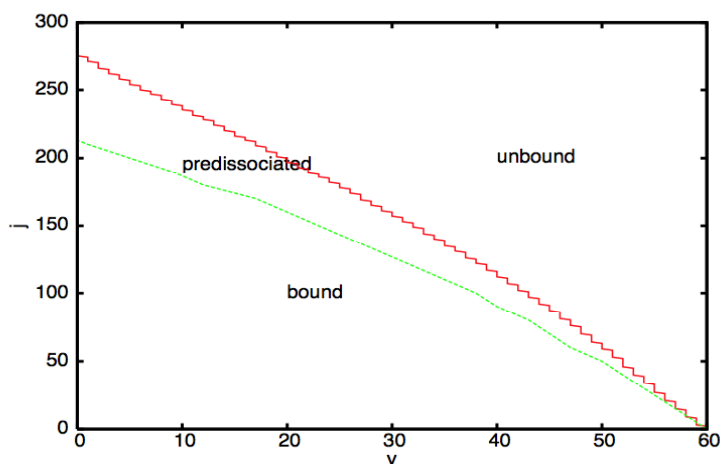
Figure 4: Rotational-vibrational levels of N_2.

Let us consider the approximation of decoupling vibration and rotation for a moment. At the very least, for this approximation to be reasonable, it is necessary for the bound v,j states of interest to fall within a rectangle in a plot such as Figure 4. This occurs for v up to about 30 and j up to about 125. This does not include any levels near dissociation. When dissociation is important, the v,j states of interest fall within a shape more like a triangle. Furthermore, decoupling vibration and rotation precludes the existence of predissociated levels. However, these levels are expected to play a very important role in dissociation. Thus for dissociation, the decoupling of vibration and rotation can not be a reasonable assumption.

2.2   N+N$_2$

We now add another particle to our mix, *e.g.* we consider our universe to consist of N and N$_2$. The solution of the electronic structure problem proceeds as for N$_2$, except now things are more complex because of the larger number of electrons and because the potential energy hypersurface now depends on three coordinates, rather than one. One interesting complication is that since the ground electronic state of the N atom is [4]S, the N$_3$ potential energy hypersurface has between 3 and 9 open shell orbitals, depending on whether the system looks more like N+N$_2$, or 3N. The large number of open shell orbitals puts considerable stresses on the software we use to compute the potential energy hypersurface. [7] In contrast to the situation with N$_2$, where we carried out electronic structure calculates and tens of geometries, for N$_3$ we carried out calculations for hundreds of geometries. An analytic representation of these calculations was then carefully formed and used for all subsequent calculations.

It is informative to consider the general topology of the potential energy hypersurface. The N$_2$ potential energy curve in Figure 2 has a single minimum at *r* about 2, and then approaches a constant as *r* goes to ∞. In contrast, the N$_3$ potential energy hypersurface has more complex structure. It has three equivalent asymptotes that look like N+N$_2$, with the three structures differing by the choice of the lone N atom. It also has three local minima that look like N-N-N with a bond angle of about 115°, which differ in the identity of the central N atom, and six local maxima which are antisymmetric distortions of the local minima that look like N—N-N or N-N—N. There are also six global minima that look like N••N-N, where •• means van der Waals interaction. The van der Waals minima are very shallow. The minimum energy pathway on the potential energy hypersurface from one N+N$_2$ structure to another involves passage from the asymptote to the van der Waals minimum, to one local maximum, N—N-N, to the local minimum N-N-N, to the next local maximum, N-N—N, to the van der Waals minimum, then on to the N$_2$+N asymptote. The overall barrier height for this process is about 3×10^1 kcal/mol, which means the likely hood of N atom exchange, as this process is called, is very low except at elevated temperatures (several thousand degrees). Finally the N$_3$ potential energy hypersurface approaches a constant, high energy as all atoms become far apart, *i.e.* forming 3N. A depiction of the potential energy hypersurface in the vicinity of the local maxima is shown in the next figure.


Figure 5: N$_3$ PES for 115°. Blue is low energy, green moderate, and red high energy.

For N+N$_2$ collisions, there are three possibilities. The N atom can simply bounce off the N$_2$ molecule, with some energy transfer between translation, rotation, and vibration. This is called an inelastic collision. The second possibility is for the trajectory to cross over from one arrangement valley, N$_a$+N$_b$N$_c$ in the

figure, to another, say $N_aN_b+N_c$. This is called an exchange reaction, and in contrast to inelastic collisions, which involves fairly limited changes to rotational and vibrational energy, exchange reaction products tend to loose memory of the initial arrangement vibrational and rotational energies and lead to very broad product distributions. The final possibility is for the trajectory to climb to the N+N+N plateau and dissociate the N_2 molecule.

How do we describe these processes? This can be done in several ways. The most rigorous way is to use quantum mechanics. This is quite expensive, but is feasible for energies below the dissociation limit. [3] Another way is to use classical mechanics for some or all of the dynamics. In our work, we will use the quasi-classical trajectory (QCT) method. [8,9] In this method, we specify a relative translational energy and v,j quantum numbers, then use old quantum mechanics to relate the quantum conditions to the initial conditions for a classical trajectory. The variables not specified by E^{rel}, v, and j, namely vibrational, rotational phases and impact parameter, are integrated over using Monte-Carlo techniques. The final state of the system is analyzed using old quantum mechanics. In general, the final values of the vibrational and rotational quantum numbers, v' and j', will not be integers. We turn them into integers by rounding them to the nearest integer. We thus obtain elementary measure of the outcome of a collision, the cross section $\sigma_{\beta\alpha}(E^{rel})$, for initial state α and final state β.[2] The cross section has units area. Although the calculation of a single trajectory is not time consuming, the number of trajectories that must be calculated is quite
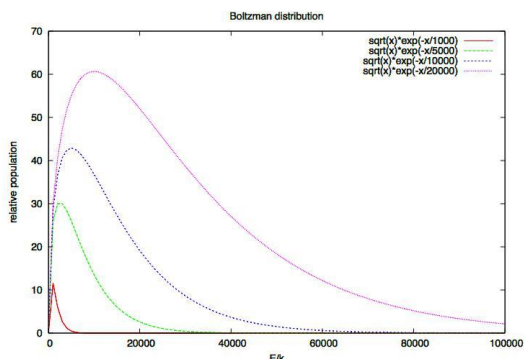

Figure 6: Energy distribution for averaging cross sections.

large. For the N+N_2 calculations presented here, nearly 10^8 trajectories were run.

Let us now consider the issue of selecting the relative translational energy E^{rel}. To compute a rate coefficient at translational temperature T^{trans}, we need to perform a Boltzman average of the average velocity times the cross section. In Figure 6 we show the (un-normalized) weighting function for the cross section for several temperatures. At low temperature, the distribution is very sharply peaked, and the most efficient way to proceed is to sample energies around the peak at each temperature. At higher temperature, the distribution becomes very broad, and it becomes more efficient to sample energies over a wide range and use them for multiple temperatures. Nonetheless, it is not necessary to converge the cross sections at high energy as much as for energies in the vicinity of the peak in the distribution, for the really high energy cross sections have only small impacts on the rate coefficients. In the present work, we use a combination of these ideas. We use Monte-Carlo sampling over E^{rel}, with an importance sampling function the speed times the Boltzman distribution at T^{trans}=20000K. We then divide the energy into 64 intervals, and take the cross section at the energy at the middle of the interval to be the average cross section we compute in that energy interval.

In Figure 7 we plot the computed dissociation rate coefficients vs. v at T^{trans}=20000K. The lines
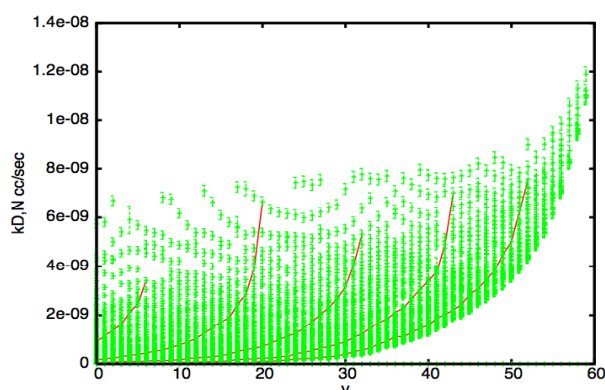
Figure 7: Dissociation rate coefficients for 20,000K.

track the v for selected values of j. We see that the largest dissociation rate coefficient occurs at the highest v for each j, with the largest dissociation rate being out of j=0, v=60. However, due to the $2j+1$ degeneracy of the rotational levels,[2] we expect much larger populations for $j >>0$, so the j=0,v=60 level is not expected to play an important role in the dissociation process. A perhaps more useful way to understand the dissociation rate data is to plot it vs. the energy difference between the top of the centrifugal barrier and the ro-vibrational energy level. Such a plot is given in the Figure 8. Now we see a much clearer pattern, with the dissociation rate showing a power law relation with the energy gap.

2.4 N_2+N_2

Now consider the universe to consist of two N_2 molecules. Now the electronic structure calculations are even more expensive, and calculations must be carried out at thousands of geometries.
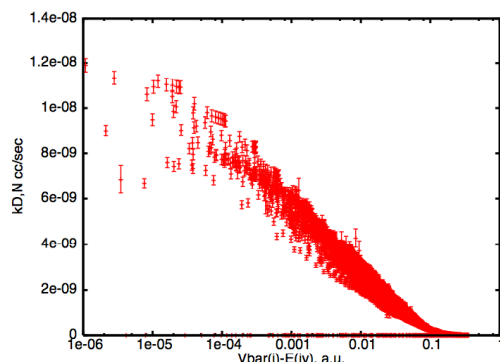
Figure 8: Dissociation rates vs. dissociation energy

Furthermore, the topology of the potential energy surface is quite complicated. Below the N_2+N+N asymptote, there exist several local minimum. One prominent one is the so-called tetrahedral (T_d) N_4 complex. This local minimum on the N_4 potential energy surface has been proposed as a high energy density material,[10] although it has not yet been synthesized in the laboratory. The significance of this

feature is if a trajectory samples this region, it will loose memory of the initial conditions and can lead to rearrangement scattering, which means unusually large vibrational and rotational energy transfer. There are also other local minima, such as the rectangle form of N_4, of which there are a number of equivalent forms. This all makes the determination of a reliable analytic representation very difficult. Our best strategy so far is illustrated in Figure 9. There we show results of electronic structure calculations for the cross or X orientation as a function of one N_2 bond length for two different values of the N_2-N_2 distance. The symbols are color coded so that green means the N_2 bond length is smaller than the N_2-N_2 distance, so the system is more like N_2+N_2, while red means larger N_2 bond lengths, so the system is more like N_2+N+N. The dark purple curve is the result of diagonalizing a 4×4 matrix, with diagonals analytic representations of potential energies of systems that look like N_2+N_2, N_2+N+N, T_d N_4, and rectangular N_4, and off diagonals being constants. For the small N_2-N_2 distance, we also show the T_d N_4 (light blue) and N_2+N+N (purple) diagonals. Although this analytic representation is still only qualitatively correct, one can clear see how the different topological features of the potential come into play.

For nuclear dynamics, we can follow the same procedure as for $N+N_2$. Now, however, quantum mechanical dynamics calculations will be possible only for quite low energy. In contrast, the QCT method can be used without much more effort per trajectory compared to $N+N_2$. Once we have finalized out N_2+N_2 potential, we will be carrying out trajectories for N_2+N_2 on a similar scale as for $N+N_2$.
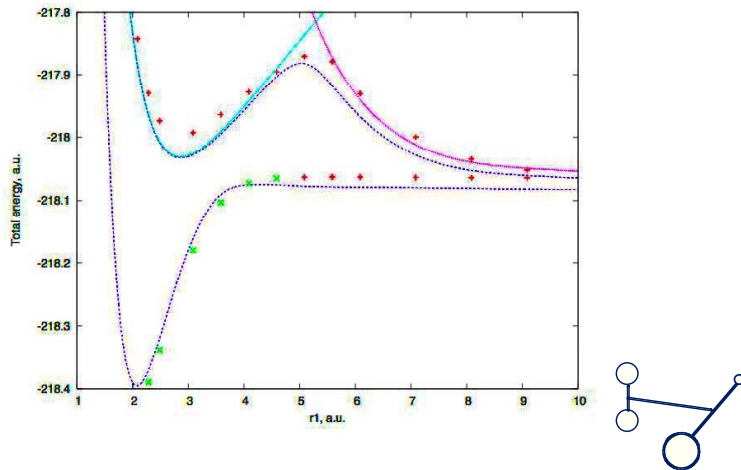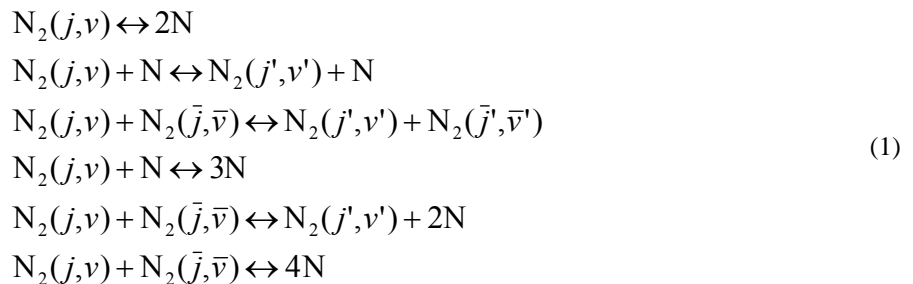
Figure 9: Cuts of N$_4$ potential in X orientation.

2.4 Gaseous N, N$_2$

We now transition from the atomic level to a macroscopic level. Once again we can take advantage of the properties of nature to simplify our simulations. As we saw, as we went from two, to three, to four atoms, our calculations got much more difficult. This will continue as we go from four to 16 to 32 ... But how far to we have to go? The unit of measure of the amount of a substance at the macroscopic level is Avogadro's number, N$_A$=6.02×10^{23}. This is the number of water molecules in a little more that one Tablespoon. This same amount of water, if allowed to evaporate at room temperature and pressure, would occupy about 22.4 liters. Avogadro's number is huge, and it will not be possible to treat this number of individual molecules. Fortunately, the fact that N$_A$ is so large also means that statistical treatments will be very accurate.[2] This means that the nature of our questions change, that is, rather than asking what the outcome of a collision is, we ask how level populations change with time. The equation we will use to describe this is the master equation.

In the master equation formulism, we assume that translational degrees of freedom equilibrate instantaneously to a distribution governed by the temperature T_{trans}. See [11] for an example of previous work by Schwenke on the H, H$_2$ system. The translational temperature can be fixed, or driven by coupling to flow equations. The solution then describes the time dependence of the concentrations for the processes

$$
\begin{aligned}
&N_2(j,v) \leftrightarrow 2N \\
&N_2(j,v) + N \leftrightarrow N_2(j',v') + N \\
&N_2(j,v) + N_2(\bar{j},\bar{v}) \leftrightarrow N_2(j',v') + N_2(\bar{j}',\bar{v}') \\
&N_2(j,v) + N \leftrightarrow 3N \\
&N_2(j,v) + N_2(\bar{j},\bar{v}) \leftrightarrow N_2(j',v') + 2N \\
&N_2(j,v) + N_2(\bar{j},\bar{v}) \leftrightarrow 4N
\end{aligned}
\tag{1}
$$

for external temperature T_{trans}, where j is the rotational quantum number and v is the vibrational quantum number. The master equation can be written in many forms, and the one we choose for Eq. (1) is

$$-\frac{dn_{jv}}{dt} = \sum_{j'v'}\left(\tilde{k}^f_{j'v'\leftarrow jv}n_{jv} - \tilde{k}^b_{jv\leftarrow j'v'}n_{j'v'}\right) - \tilde{k}^R_{jv}n_N^2$$

$$-\frac{1}{2}\frac{dn_N}{dt} = \sum_{jv}\left(\tilde{k}^f_{jv}n_N^2 - \tilde{k}^b_{jv}n_{jv}\right)$$

(2)

where n_{jv} is the concentration of $N_2(j,v)$, n_N is the concentration of N atoms, the sums are over all bound and all long lived metastable levels of N_2, and the $\tilde{k}$ are pseudo first or second order rate coefficients defined as

$$\tilde{k}^f_{j'v'\leftarrow jv} = \delta_{j'j}\delta_{v'v}\left[k^{PD}_{jv} + k^{D,N}_{jv}n_N + \sum_{\bar{j}\bar{v}}\left(1 + \delta_{\bar{j}j}\delta_{\bar{v}v}\right)k^{DD}_{jv\bar{j}\bar{v}}n_{\bar{j}\bar{v}}\right] + k^{ET,N}_{j'v'\leftarrow jv}n_N$$
$$+ \sum_{\bar{j}'\bar{v}'\bar{j}\bar{v}}\left(1 + \delta_{\bar{j}j}\delta_{\bar{v}v}\right)k^{ET,N_2}_{j'v'\bar{j}'\bar{v}'\leftarrow jv\bar{j}\bar{v}}n_{\bar{j}\bar{v}} + \sum_{\bar{j}\bar{v}}\left(1 + \delta_{\bar{j}j}\delta_{v'v}\right)k^{D,N_2}_{j'v'\leftarrow jv\bar{j}\bar{v}}n_{\bar{j}\bar{v}},$$

(3)

$$\tilde{k}^b_{jv\leftarrow j'v'} = k^{ET,N}_{jv\leftarrow j'v'}n_N + \sum_{\bar{j}'\bar{v}'\bar{j}\bar{v}}\left(1 + \delta_{\bar{j}j}\delta_{\bar{v}v}\right)k^{ET,N_2}_{jv\bar{j}\bar{v}\leftarrow j'v'\bar{j}'\bar{v}'}n_{\bar{j}'\bar{v}'} + \sum_{\bar{j}\bar{v}}\left(1 + \delta_{\bar{j}j}\delta_{\bar{v}v}\right)k^{R,N_2}_{jv\bar{j}\bar{v}\leftarrow j'v'}n_N^2,$$

(4)

$$\tilde{k}^R_{jv} = k^{TR}_{jv} + k^{R,N}_{jv}n_N + \sum_{\bar{j}\bar{v}}\left(1 + \delta_{\bar{j}j}\delta_{\bar{v}v}\right)k^{DR}_{jv\bar{j}\bar{v}}n_N^2,$$

(5)

$$\tilde{k}^f_{jv} = k^{TR}_{jv} + \sum_{j'v'\bar{j}\bar{v}}k^{R,N_2}_{jv\bar{j}\bar{v}\leftarrow j'v'}n_{j'v'} + k^{R,N}_{jv}n_N + 2\sum_{\bar{j}\bar{v}}k^{DR}_{jv\bar{j}\bar{v}}n_N^2,$$

(6)

$$\tilde{k}^b_{jv} = k^{PD}_{jv} + k^{D,N}_{jv}n_N + \sum_{j'v'\bar{j}\bar{v}}k^{D,N_2}_{j'v'\leftarrow jv\bar{j}\bar{v}}n_{\bar{j}\bar{v}} + 2\sum_{\bar{j}\bar{v}}k^{DD}_{jv\bar{j}\bar{v}}n_{\bar{j}\bar{v}},$$

(7)

where δ_{nm} is unity if n=m and zero otherwise, k^{ET} is an energy transfer rate coefficient, k^D is an
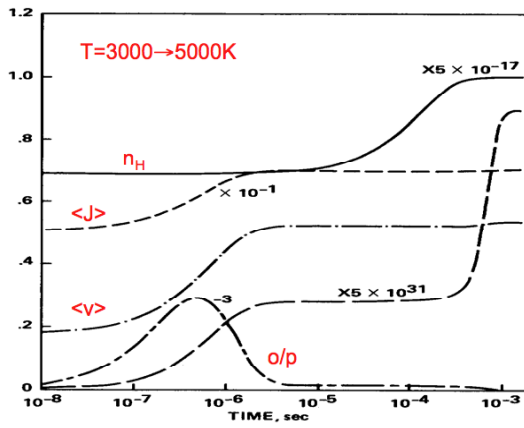

FIG. 3. Same as Fig. 2 except $C^{Tot} = 10^{16}$ molecules/cc.

Figure 10: populations for H, H$_2$ from master equation.

dissociation rate coefficient, k^R is an recombination rate coefficient, k^{PD} is a predissociation rate coefficient, k^{TR} is a tunnelling recombination rate coefficient, k^{DD} is a double dissociation rate coefficient, and k^{DR} is a double recombination rate coefficient. The predissociation and tunnelling recombination rate coefficients are nonzero only for metastable jv levels. Since N$_2$ has 9390 jv levels, this means for the N, N$_2$ system there will 9391 coupled ordinary differential equations, thus the solution of the master equation will be very arduous.

For an example of what can be learned from a master equation study coupled with accurate state-to-state rate coefficients, readers are referred to Ref. 11. Here we studied the H, H$_2$ system. This system shares a great deal with the N, N$_2$ system, except the fact that H$_2$ has only 348 jv levels makes the solution of the master equation much easier. In Figure 10 we show populations as a function of time for a 2000K temperature jump. This figure is a distillation of a vast amount of data, yet we see some very interesting aspects of the dissociation of H$_2$. First we note that the average value of j and v equilibrate at about the same rate, reaching their final values by a few µsec. In contrast, dissociation does not begin to occur until about 10 µsec, with vibrational and rotation in equilibrium. Now the different vibrational rotational spacings, potential energy surfaces, and temperatures for the N,N$_2$ system will be different from the H, H$_2$ system, so this decoupling of time scales may not occur in our system, but this remains a very tantalizing result.

A serious difficulty addressed in Ref.[11] was how to compare the master equation simulations to experiment. This is because, *e.g.*, experimental measurements report the rate k^D in the expression

$$-\frac{dn_{N_2}}{dt} = k^D(n_{N_2} - n_N^2/K^{eq}) \tag{8}$$

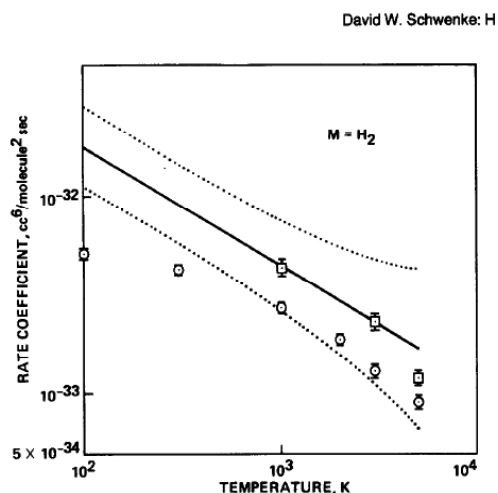and the master equation can not be analytically reduced to this form. Therefore k^D is known as the

David W. Schwenke: H

FIG. 8. Comparison of the current results for k^{3bdy,H_2} ($\square$), to previous (Ref. 1) ORT results (O) and the experimental recommendation of Ref. 3 (solid line). The dotted line demarcates the experimental error limit.

Figure 11: Comparison between calculated and experimental recombination rate coefficients for H$_2$.

phenomenological rate coefficient because although the rate law of Eq. (8) is observed, it can not be derived from more accurate theory. To compare to experiment, we considered methods based on three broad ideas: (i) data fitting, (ii) equilibrium one way flux, and (iii) eigenvalue analysis.

In the data fitting approach, we closely mimicked experiment by determining the time dependence of the N and aggregate N_2 concentrations, and then determining the best k^D that reproduced the time profile when we used Eq. (8). In Figure 11 we show the comparison with experiment that we obtained. The results were very good. It should be noted that the apparent deterioration at the highest temperature is just simply a reflection on the uncertainty in determining the rate coefficient since at these temperatures, the equilibrium faction of H_2 is very small.

The next scheme we used to extract the phenomenological rate coefficient was the equilibrium one-way flux method. This was not nearly as reliable a method, being only capable of order of magnitude predictions of the recombination rate coefficient. Nevertheless this will give valuable insight into the dissociation process. In this method, we evaluate the rhs of Eq. (2) using equilibrium concentrations and only include terms leading to dissociation. We show the contribution of the various terms as a function of v in Figure 13 and as a function of j in Figure 12. We see that the dissociation rate is dominated by low v and high j.
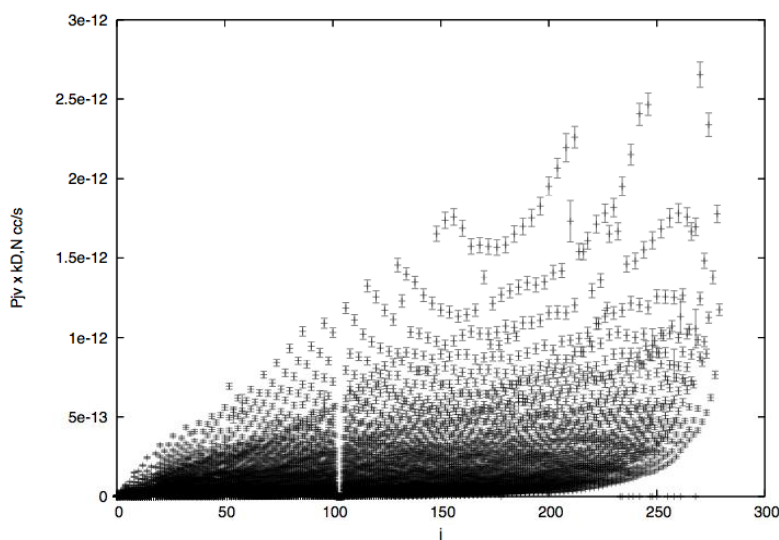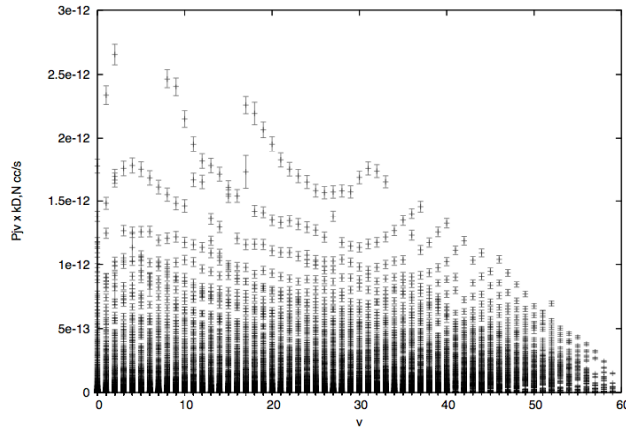

Figure 12: Equilibrium dissociation flux at 20,000K.

Figure 13: Equilibrium dissociation flux at 20,000K.

We next turn to the eigenvalue analysis method. For H_2, it proved to be a very accurate and efficient method. In this method, we observe that we can write the master equation in the form

$$\frac{d\vec{n}}{dt} = \mathbf{C}(\vec{n})\vec{n} = \mathbf{C}(\vec{n}^f)\vec{n} + ... \tag{9}$$

where bold means matrix and the superscript f means final. That is, we linearize the master equation. Then the solution can be found in terms of the eigenvalues and eigenvectors of the matrix $\mathbf{C}$:

$$n_\alpha(t) = n_\alpha^f + \sum_\beta V_{\alpha\beta} c_\beta \exp \lambda_\beta t \tag{10}$$

Then the phenomenological rate coefficient is computed from the first nonzero eigenvalue. The problem with this procedure for the N_2 system is that $\mathbf{C}$ is a 9391×9391 non-symmetric matrix, and good canned routines to determine the lowest eigenvalues and eigenvectors of a matrix of this size do not exist. But this can be overcome by the following technique: if we multiply $\mathbf{C}$ from the right by the diagonal matrix made up of the square roots of the n_α^f and then multiply the result from the left with the inverse of this diagonal matrix, then we obtain a new matrix which is made up of a 9390×9390 symmetric part, and then one row and one column which are not symmetric. We can then diagonalize the symmetric part efficiently, determining only the eigenvalues of interest, and then use the non-symmetric Jacobi method to clean up the rest to yield the eigenvalues of interest. Thus we expect this to be a very promising method for treating the full system.

3.0 MODELING

Finally let us ask the question of what is it that computational fluid dynamics actually needs for accurate simulations. Clearly following the populations of all 9390 vj levels is a vast overkill and also prohibitatively expensive. What is actually needed are the N, and N_2 number densities, to go into the mass conservation equations, the average internal energies, to go into the energy conservation equations, and finally the internal state distribution, to go into the radiation transfer equations. The eigenvalue analysis method gives all this information, except the eigenvalues and eigenvectors depend on T^{trans}, the total density and the particular mixture. Thus a more flexible method is required.

Let us suppose that all the vj state number densities are not independent, *i.e.*

$$n_\alpha(t) = x_1(t)n_\alpha^0, \ \alpha = 1,...,N_1$$
$$n_\alpha(t) = x_2(t)n_\alpha^0, \ \alpha = N_1 + 1,...,N_2 \tag{11}$$

etc. Then can we determine how the x depend on time? This technique is known as lumping, and can be written mathematically as follows: let

$$\dot{x} = \mathbf{M}\dot{n} \tag{12}$$

where $\mathbf{M}$ is some invertible 9391×9391 matrix. Then the governing equation for the x is

$$\frac{d\dot{x}}{dt} = \mathbf{K}\overset{\mathbf{r}}{x} \tag{13}$$

with

$$\mathbf{K} = \mathbf{MCM}^{-1} \tag{14}$$

So far this has just introduced a large amount of extra work, but now make the approximation that $x_i=0$ for all time for $i>m, m<<9391$. This converts the master equation into one having only m coupled equations. The advantage of this method is by performing a significant amount of work up front to determine the rate equations for the lumps, we can recover accurate time dependent populations from a much smaller set of equations.

What are some ways to choose the lumps? One choice is to have m run 0 to 60 and represent the vibrational levels with the j populations be Boltzman at some temperature, say T^{trans}. This is a perfectly well defined and reasonable proposition, provided the j levels are those for the particular v. Thus we can eliminate the j levels, as we would like to do, but note that this is not the same is decoupling vibration and rotation. Some other lumping schemes are to sort jv levels by energy, and include in a lump all levels with similar energies. This has the advantage that the populations within the lump will be primarily determined by degeneracy factors, rather than an external temperature. Another idea would be to carry out the eigenvalue analysis for a series of likely situation, and then use the eigenvectors to define the lumps. And of course, other ideas are possible.

4.0 CONCLUSIONS

I have outlined the procedure involved from going from a first principle treatment of molecular dissociation to a model for use in CFD calculations. There are a multitude of complex problems that must be solved before a viable model is developed. Our goal is to use the first principle data to determine a hierarchal set of models that can be used in CFD calculations. These models will have wide applicability, and systematically trade off between accuracy and expense.

5.0 ACKNOWLEDGEMENTS

REFERENCES

[1]   Park, C, *Nonequilibrium Hypersonic Aerothermodynamics*, Wiley, New York, 1990.

[2]   Atkins, P.W. and Friedman, R.S., *Molecular Quantum Mechanics*, Oxford University Press, Oxford, 1997.

[3]   Wang, D., Huo W.M., Dateo, C.E., Schwenke, D.W., Stallcop, J.R., "Quantum study of the N+N_2 exchange reaction: State-to-state reaction probabilities, initial state selected probabilities, Feshbach resonances, and product distributions", *J. Chem. Phys.*, Vol. 120, 2004, pp. 6041

[4]   Goldstein, H., *Classical Mechanics*, Addison Wesley, Reading, 1980.

[5]   Einstein, A.*Ver. Deut. Phys. Ges.*, Vol. 19, 1917, pp. 82; Brillouin, L. *J. Phys.*, Vol. 7, 1926, pp. 353; Keller, J., *Ann. Phys.*, Vol. 4, 1958, pp. 180

[6]   LeRoy, R. J., Huang, Y., and Jary, C.,"An accurate analytic potential function for ground-state N_2 from a direct-potential-fit analysis of spectroscopic data," *J. Chem. Phys.*, Vol. 125, 2006, pp. 165410

[7]   MOLPRO is a package of ab initio programs written by H.-J. Werner, P. J. Knowles, R. Lindh, F. R. Manby, M. Schütz, P. Celani, T. Korona, A. Mitrushenkov, G. Rauhut, T. B. Adler, R. D. Amos, A. Bernhardsson, A. Berning, D. L. Cooper, M. J. O. Deegan, A. J. Dobbyn, F. Eckert, E. Goll, C. Hampel, G. Hetzer, T. Hrenar, G. Knizia, C. Köppl, Y. Liu, A. W. Lloyd, R. A. Mata, A. J. May, S. J. McNicholas, W. Meyer, M. E. Mura, A. Nicklaß, P. Palmieri, K. Pflüger, R. Pitzer, M. Reiher, U. Schumann, H. Stoll, A. J. Stone, R. Tarroni, T. Thorsteinsson, M. Wang, A. Wolf .

[8]   Truhlar, D.G. and Muckerman, J. T., in *Atom-Molecule Collision Theory*, pp. 505 ed. by Bernstein, R.B., Plenum, New York, 1979.

[9]   Schwenke, D.W., "Calculation of ate constants for the three-body recombination H_2 in the presence of H_2", *J. Chem. Phys.*, Vol. 89, 1988 pp. 2076

[10]   See, *e.g.* Lee, T.J. and Martin, J. M. L., "An accurate quartic force field, fundamental frequencies, and binding energy for the high energy density material T_dN_4," *Chem. Phys. Lett.,* Vol. 357, No. 4, 2002, pp. 319-325.

[11]   Schwenke, D. W., "A theoretical prediction of hydrogen molecule dissociation-recombination rates including an accurate treatment of internal state nonequilibrium effects," *J. Chem. Phys.*, Vol. 92, No. 8, 1990, pp. 7267-7282